

Reactions of Thorium Atoms with Polyhalomethanes: Infrared Spectra of the $\text{CH}_2=\text{ThX}_2$, $\text{HC}\div\text{ThX}_3$, and $\text{XC}\div\text{ThX}_3$ Molecules

Jonathan T. Lyon^[a] and Lester Andrews^{*[a]}

Keywords: Thorium / Matrix infrared spectra / Density functional calculations / Methylidene / Methylidyne

Laser-ablated thorium atoms react with methylene fluoride to form singlet $\text{CH}_2=\text{ThF}_2$, with fluoroform to give triplet $\text{HC}\div\text{ThF}_3$, and with CF_4 to produce triplet $\text{FC}\div\text{ThF}_3$ molecules as the major products trapped in solid argon. Infrared spectroscopy, isotopic substitution, and density functional theoretical calculations confirm the identity of these methylidene and methylidyne complexes. Parallels with the analogous chloromethane and Group 4 metal reaction products are discussed. Structure calculations show that the $\text{C}=\text{Th}$ bond lengths decrease and the agostic distortion increases from $\text{CH}_2=\text{ThF}_2$ to $\text{CH}_2=\text{ThFCl}$ to $\text{CH}_2=\text{ThCl}_2$ for the methylidene complexes. The triplet-state $\text{HC}\div\text{ThF}_3$ and $\text{FC}\div\text{ThF}_3$ elec-

tron-deficient methylidyne complexes exhibit delocalized π -bonding as evidenced by spin densities comparable to those calculated for the analogous zirconium complexes. Chlorine substitution for fluorine supports stronger $\text{C}\div\text{Th}$ bonds. Thus, thorium appears to react as the early transition-metal atoms with fluoro- and chloromethanes. However, there is a substantial contribution from Th 5f orbitals in addition to 6d in the SOMO forming the weak π -bonds in these electron-deficient methylidyne complexes.

(© Wiley-VCH Verlag GmbH & Co. KGaA, 69451 Weinheim, Germany, 2008)

Introduction

A large number of alkylidene complexes with Group 4 metals have been investigated for applications as catalysts in alkene metathesis and alkane activation reactions,^[1–4] but the analogous (alkylidene)actinide complexes have not been prepared.^[1–5] Some related uranium–carbon multiple-bonded complexes and surface-stabilized (alkylidene)actinide species have been investigated.^[6,7] Hence, it is of interest to prepare simple (methylidene)actinide complexes for comparison to Group 4 analogs. In this regard, we have formed $\text{CH}_2=\text{ThH}_2$ from the Th and CH_4 reaction and $\text{CH}_2=\text{ThHX}$ from the corresponding methyl halide reactions, and our B3LYP calculations find an agostic distortion near that computed for the analogous methylidene Group 4 complexes.^[8–10] Analogous Group 4 reactions with methylene halide precursors supported α -halogen transfer and gave the expected $\text{CH}_2=\text{MX}_2$ methylidene complexes, which showed no agostic distortion, and the haloforms and CX_4 precursors produced instead an interesting new class of electron-deficient triplet-state methylidyne complexes $\text{HC}\div\text{MX}_3$ and $\text{XC}\div\text{MX}_3$ involving extensive α -halogen transfer.^[11–13] With mixed fully halogenated fluorochloromethanes, two different complexes were formed with two competitive α -halogen transfer processes.^[14] We wish to report here experiments and calculations on the polyhalogen-

substituted (methylidene)thorium complexes prepared from methylene halides, and the corresponding electron-deficient methylidyne complexes synthesized from haloforms and carbon tetrahalides. We are particularly interested in comparing the physical characteristics of the analogous thorium and Group 4 complexes. Results on the chiral $\text{CH}_2=\text{ThFCl}$ complex have been reported in a preliminary communication.^[15]

Experimental and Theoretical Methods

Experimentally, laser-ablated Th atoms were reacted with the CH_2F_2 , CHF_3 , CF_4 , CH_2Cl_2 , CHCl_3 , CCl_4 , CH_2FCl , CHF_2Cl , CHFCl_2 , CF_3Cl and CF_2Cl_2 molecules and selected isotopic modifications (Du Pont, Peninsular, Fisher) in excess argon (0.5–1 % concentrations) during condensation onto an 8 K cesium iodide window as described previously.^[13,14,16,17] Infrared spectra were recorded with a Nicolet 550 spectrometer after sample deposition, after annealing, and after irradiation by a common mercury arc street lamp. Theoretically, the structures and vibrational frequencies of the thorium product complexes were calculated using the Gaussian 98 program employed for the analogous Group 4 complexes.^[10,18] Here the B3LYP functional was used with the medium 6-311++G(2d,p) basis set, and relativistic effects were included in the SDD pseudopotential for thorium (30 valence electrons).^[19,20] The vibrational frequencies were computed analytically, and zero-point energy was included in the calculation of relative product energies.

[a] Department of Chemistry, University of Virginia, P. O. Box 400319, Charlottesville, Virginia 22904-4319, USA
E-mail: lsa@virginia.edu

Supporting information for this article is available on the WWW under <http://www.eurjic.org> or from the author.

Results and Discussion

Reactions of laser-ablated Th atoms with the methylene halide, haloform, and tetrahalomethane precursors involving fluorine and chlorine during condensation in excess argon will be described in turn. These experiments also produced transient free-radical and molecular ion absorptions from the precursor, which are common to different metals and have been identified previously.^[21–23] In addition, weak bands were observed for thorium oxides.^[16]

CH₂X₂

The thorium and CH₂F₂ reaction gives four new infrared absorptions at 653.4, 643.2, 509.6, and 497.0 cm^{−1}, which are compared in Table 1 with frequencies calculated for the major product of this reaction. The last two bands exhibit major site splittings at 511.0 and 501.0 cm^{−1}, which are important as they confirm the small isotopic shifts observed on the major bands as given in Table 1. The infrared spectra are shown in Figure 1 where the above absorptions are marked by arrows. Irradiation with near ultraviolet light ($\lambda > 290$ nm pyrex filter and the full mercury arc $\lambda > 220$ nm, unfiltered) increased these bands slightly, and annealing to 30 K sharpened the absorptions. Isotopic spectra are illustrated in Figure 1: the bottom set is natural abundance precursor, the middle set is ¹³CH₂F₂, and the top set is CD₂F₂.

Density functional theory calculations are helpful for identifying the reaction products according to recent work with Ti, Zr and Hf.^[11–14] Our B3LYP calculation found the approximately symmetrical structure illustrated in Figure 2 and antisymmetric and symmetric Th–F stretching modes for singlet ground-state CH₂=ThF₂ complex at 515.5 and 520.6 cm^{−1} as listed in Table 1. [The triplet state is 1 kcal/mol higher in energy and has much lower CH₂ wagging (578 cm^{−1}) and C–Th stretching (471 cm^{−1}) mode predictions.] The calculated singlet-state frequencies are slightly higher than the strongest observed bands at 509.6 and 497.0 cm^{−1} and in the region expected for Th–F vibrations (518.6 cm^{−1} for CH₂=ThHF and 520 cm^{−1} for ThF₄).^[9,24]

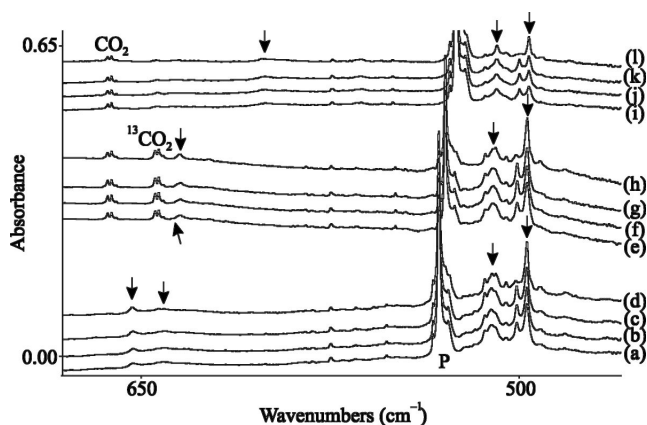


Figure 1. Infrared spectra in the 670–470 cm^{−1} region for laser-ablated Th atoms co-deposited with CH₂F₂ in excess argon at 8 K. (a) Th and 1% CH₂F₂ in argon co-deposited for 1 h, (b) after >290 nm irradiation, (c) after >220 nm irradiation, and (d) after annealing to 30 K. (e) Th and 0.8% ¹³CH₂F₂ in argon co-deposited for 1 h, (f) after >290 nm irradiation, (g) after >220 nm irradiation, and (h) after annealing to 30 K. (i) Th and 1% CD₂F₂ in argon co-deposited for 1 h, (j) after >290 nm irradiation, (k) after >220 nm irradiation, and (l) after annealing to 30 K. P denotes methylene fluoride precursor absorptions.

Furthermore, the small observed and calculated ¹³C and D shifts for these bands substantiates their assignments as Th–F stretching modes. The sharp 653.4 cm^{−1} band shifts 18.7 cm^{−1} with ¹³C and 51.3 cm^{−1} with D, and the calculated shifts for the C=Th stretching mode at 630.1 cm^{−1} are 17.3 and 50.2 cm^{−1}, which is a very good agreement considering the approximations involved.^[9–14,25,26] The broader 643.2 cm^{−1} band is appropriate for the CH₂ wagging mode calculated at 667.7 cm^{−1} because it is near this mode for analogous complexes at 634.6 cm^{−1} (CH₂=ThH₂) and at 634.0 cm^{−1} (CH₂=ThHF).^[8,9] Our B3LYP calculation predicts the wagging mode very well, but it undershoots the C=Th stretching mode. The ¹³C counterpart is observed as a shoulder absorption at 636 cm^{−1}, but the D counterpart is shifted into the strong parent band region near 500 cm^{−1}. The correlation of the four strongest calculated and observed infrared absorptions with isotopic shifts substanti-

Table 1. Observed and calculated fundamental frequencies of CH₂=ThF₂ in the singlet ground electronic state.^[a]

Approximate Mode Description	CH ₂ =ThF ₂			¹³ CH ₂ =ThF ₂			CD ₂ =ThF ₂		
	Obsd. ^[b]	Calcd.	Int.	Obsd. ^[b]	Calcd.	Int.	Obsd. ^[b]	Calcd.	Int.
CH stretch		3087.2	12		3075.7	12		2286.9	2
CH stretch		3012.6	13		3006.9	13		2186.2	2
CH ₂ bend		1315.1	2		1307.9	2		1003.9	14
CH ₂ wag	643.2	667.7	182	636sh	661.7	176	— ^[c]	524.6	165
C=Th stretch	653.4	630.1	45	634.7	612.8	36	602.1	579.9	13
Th–F stretch	511.0, 509.6	520.6	123	510.7, 509.2	519.1	127	—, 509.1	513.2	109
Th–F stretch	501.0, 497.0	515.5	227	500.8, 496.9	515.4	226	500.0, 496.2	514.9	222
CThH bend		387.5	0		387.2	0		279.5	0
CH ₂ twist		208.4	15		203.8	14		192.0	15
CH ₂ rock		113.6	10		112.8	10		111.0	9
deformation		80.2	27		80.0	26		79.2	25
FThF bend		60.6	0		60.5			45.8	0

[a] Frequencies and calculated intensities are in cm^{−1} and km/mol, calculated using B3LYP/6-311++G(2d,p)/SDD. [b] Observed in argon matrix, the stronger absorption is in bold type. [c] Masked by CD₂F₂ precursor.

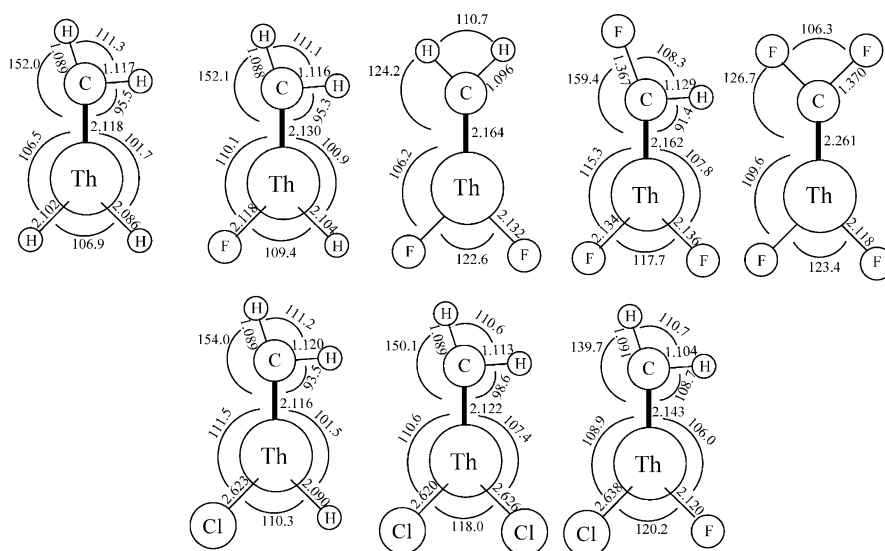


Figure 2. Optimized molecular structures [B3LYP/6-311++G(2d,p)/SDD] for (methylidene)thorium complexes $CX_2=ThX_2$ ($X = H, F, Cl$). Bond lengths are in Å and angles are in °.

ates this identification of the $CH_2=ThF_2$ methylidene complex. The observed/calculated frequency fit for $CH_2=ThF_2$ is almost as good as found for the analogous $CH_2=ThHF$ complex.^[9]

Additional MP2 and BPW91 calculations^[18] were performed as these methods favor the agostic interaction.^[27] We found a symmetrical minimum-energy $CH_2=ThF_2$ structure with MP2 almost the same as shown in Figure 2, and an isoergic asymmetrical minimum with 0.012 Å shorter C=Th bond and 101.4° and 146.2° H–C–Th bond angles, and the BPW91 functional gave a result similar to the latter, 0.014 Å shorter C=Th bond and 105.5° and 143.4° bond angles, near that found with the PW91 functional.^[15] The BPW91 functional also predicted the correct order of the CH_2 wag and C=Th stretching modes. Likewise, higher level calculations will be required to determine if the agostic interaction is stronger with thorium than the Group 4 metals to provide agostic distortion in $CH_2=ThF_2$. However, a very recent CASSCF/CASPT2 calculation found that the agostic distortion in $CH_2=ThH_2$ is less than that in $CH_2=ZrH_2$, a result in agreement with density functional theory predictions.^[8,10,28]

The reaction, based on a large body of previous evidence,^[10] is believed to proceed first through the triplet insertion product CH_2F-ThF , which is 119 kcal/mol lower in energy than the $Th + CH_2F_2$ reagents, to the most stable product of this stoichiometry, namely singlet $CH_2=ThF_2$ formed by α -F transfer, which is 198 kcal/mol lower in energy than the reagents [the corresponding triplet CH_2-ThF_2 is 16 kcal/mol higher in energy]. The corresponding α -H transfer singlet methylidene $CHF=ThHF$ is 71 kcal/mol higher in energy than $CH_2=ThF_2$, and even though α -H transfer is surely faster than α -F transfer, the latter produces by far the more stable complex. Finally, the triplet complex formed by another α -H transfer, namely $HC-ThHF_2$, is 36 kcal/mol higher in energy than the most

stable singlet $CH_2=ThF_2$ complex observed here. Thus, the favorable reaction [Equation (1)] is exothermic by 198 kcal/mol at the B3LYP level of theory, and the reaction stops at the methylidene complex.



Experiments with dichloromethane gave strong 675.6 cm^{-1} (668.7 cm^{-1} matrix site splitting) and weaker, broad 652.2 cm^{-1} absorptions, which increased 20% on >290 nm irradiation. These bands shifted to 654.7 cm^{-1} and to approximately 647 cm^{-1} not resolved from the 648.4 cm^{-1} site splitting and $^{13}CO_2$ impurity in the ^{13}C sample, and to 618.8 and 514.5 cm^{-1} with CD_2Cl_2 as shown in Figure 3. The observed ^{13}C shifts (20.9 and 5 cm^{-1}) and the medium and large D shifts are appropriate for C=Th stretching and CH_2 wagging motions, respectively. The similar $CH_2=ThHCl$ complex exhibited these absorptions at 682.0 and 643.0 cm^{-1} in excellent agreement with the prediction of B3LYP calculations.^[9] The common C=Th stretch and CH_2 wag are 23 and 9 cm^{-1} higher for $CH_2=ThCl_2$ than for $CH_2=ThF_2$, which is similar to the relationship between $CH_2=ThHF$ and $CH_2=ThHCl$. However, the $CH_2=ThCl_2$ complex converges to an asymmetric minimum with no imaginary frequencies and a symmetrical minimum 0.1 kcal/mol lower in energy with a 152 cm^{-1} imaginary frequency. Both calculations predict the C=Th stretching and CH_2 wagging modes in this region with D shifts comparable to those observed, which are compared in Table 2 for the asymmetric structure. We find a similar asymmetric structure using the BPW91 functional with slightly smaller agostic angle and shorter C–Th bond (96.0° and 2.115 Å). Although the BPW91 functional undershoots the C=Th stretching and CH_2 wagging modes (657 and 629 cm^{-1}), it does predict their order correctly (Table S2, Supporting Information). In addition, we started an MP2 calculation at the symmetric minimum, and it converged to

Table 2. Observed and calculated fundamental frequencies of $\text{CH}_2=\text{ThCl}_2$ in the singlet ground electronic state.^[a]

Approximate mode	$\text{CH}_2=\text{ThCl}_2$			$^{13}\text{CH}_2=\text{ThCl}_2$			$\text{CD}_2=\text{ThCl}_2$		
Description	Obsd. ^[b]	Calcd.	Int.	Obsd. ^[b]	Calcd.	Int.	Obsd. ^[b]	Calcd.	Int.
CH stretch		3134	1		3124	2		2315	2
CH stretch		2889	11		2882	11		2105	3
CH_2 bend		1334	25		1326	23		1019	34
C=Th stretch	675.6	677.5	109	654.7	656.9	120	618.8	613	88
CH_2 wag	652.2	667.0	159	647	661.5	136	514.5	522	113
Th–Cl stretch	— ^[c]	352	2	— ^[c]	352	1	— ^[c]	314	131
Th–Cl stretch	— ^[c]	326	89	— ^[c]	325	91	— ^[c]	311	41
CThH bend		310	53		310	53		258	1
CH_2 twist		291	32		290	29		230	1
CH_2 rock		135	4		132	4		120	3
Deformation		80	6		79	6		77	5
ClThCl bend		51	14		51	14		50	13

[a] Frequencies and calculated intensities are in cm^{-1} and km/mol , calculated using B3LYP/6-311++G(2d,p)/SDD. [b] Observed in argon matrix. [c] Below our instrumental limit.

the same asymmetric structure, and we did likewise for the asymmetric minimum and this structure converged. Finally, we illustrate the asymmetrical structure in Figure 2, but we found the Group 4 analogs to be symmetrical.^[12] Higher levels of theory will be required to settle the question of agostic distortion for the $\text{CH}_2=\text{ThCl}_2$ complex,^[27] but it appears that the C–Th bond is shorter in the chloride complex and supports the agostic interaction, which does not happen in the $\text{CH}_2=\text{ThF}_2$ complex with a slightly longer C–Th bond.

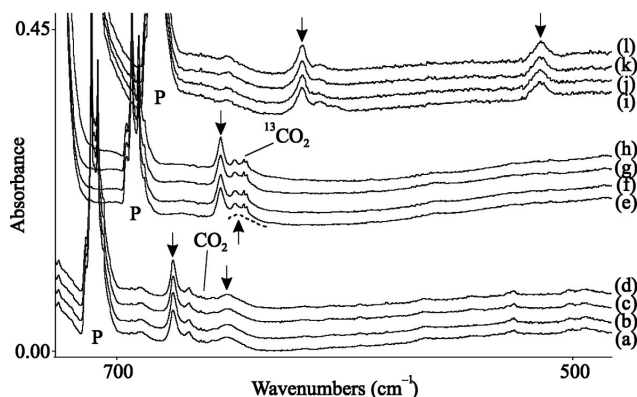


Figure 3. Infrared spectra in the 670–470 cm^{-1} region for laser-ablated Th atoms co-deposited with CH_2Cl_2 in excess argon at 8 K. (a) Th and 1% CH_2Cl_2 in argon co-deposited for 1 h, (b) after >290 nm irradiation, (c) after >220 nm irradiation, and (d) after annealing to 30 K. (e) Th and 1% $^{13}\text{CH}_2\text{Cl}_2$ in argon co-deposited for 1 h, (f) after >290 nm irradiation, (g) after >220 nm irradiation, and (h) after annealing to 30 K. (i) Th and 1% CD_2Cl_2 in argon co-deposited for 1 h, (j) after >290 nm irradiation, (k) after >220 nm irradiation, and (l) after annealing to 30 K. P denotes dichloromethane precursor absorptions.

In order to examine the agostic distortion as a function of the number of fluorine substituents, we prepared the mixed $\text{CH}_2=\text{ThFCl}$ methyldiene complex. Infrared spectra

are illustrated in Figure 4. The natural isotopic species exhibited new absorptions at 668.0, 647.1, and 516.2 cm^{-1} , which shifted to 648.3, 642.9, and 516.1 cm^{-1} with $^{13}\text{CH}_2\text{FCl}$. The deuterium counterparts were observed at 614.2, 496.2, and 516.0 cm^{-1} . The product absorptions increased slightly on UV irradiation and sharpened on 30 K annealing following the behavior of the pure fluorine and chlorine derivatives. Our B3LYP calculation for $\text{CH}_2=\text{ThFCl}$ found a distorted complex, intermediate between the pure fluorine and chlorine species (Figure 2). We conclude from this that lone-pair repulsions are not the major factor affecting agostic distortion, but the inductive effect of the halogen substituents reduces the metal valence orbital size and overlap with carbon and increases the bond length, which decreases the agostic interaction. Table 3

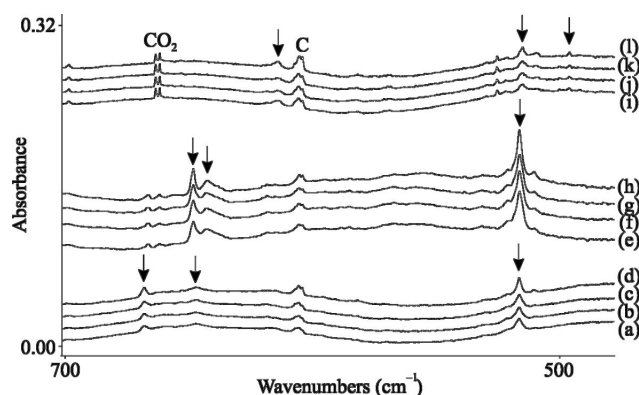


Figure 4. Infrared spectra in the 680–480 cm^{-1} region for laser-ablated Th atoms co-deposited with CH_2FCl in excess argon at 8 K. (a) Th and 1% CH_2FCl in argon co-deposited for 1 h, (b) after >290 nm irradiation, (c) after >220 nm irradiation, and (d) after annealing to 30 K. (e) Th and 1% $^{13}\text{CH}_2\text{FCl}$ in argon co-deposited for 1 h, (f) after >290 nm irradiation, (g) after >220 nm irradiation, and (h) after annealing to 30 K. (i) Th and 1% CD_2FCl in argon co-deposited for 1 h, (j) after >290 nm irradiation, (k) after >220 nm irradiation, and (l) after annealing to 30 K. C denotes common absorption in thorium experiments.

Table 3. Observed and calculated fundamental frequencies of $\text{CH}_2=\text{ThFCl}$ in the singlet ground electronic state.^[a]

Approximate Mode Description	$\text{CH}_2=\text{ThFCl}$			$^{13}\text{CH}_2=\text{ThFCl}$			$\text{CD}_2=\text{ThFCl}$		
	Obsd. ^[b]	Calcd.	Int.	Obsd. ^[b]	Calcd.	Int.	Obsd. ^[b]	Calcd.	Int.
CH stretch		3114.2	4		3103.8	5		2301.3	2
CH stretch		2961.3	11		2954.5	12		2155.2	2
CH_2 bend		1320.2	12		1312.7	10		1009.8	27
$\text{C}=\text{Th}$ stretch	668.0	649.4	81	648.3	630.5	75	614.2	590.4	55
CH_2 wag	647.1	670.3	170	642.9	664.4	164	496.2	524.2	107
Th–F stretch	516.2	530.3	171	516.1	529.8	172	516.0	528.5	191
Th–Cl stretch		369.3	2		369.1	2		264.9	1
CThH bend		305.3	88		305.0	87		305.2	86
CH_2 twist		192.1	7		188.0	7		174.8	8
CH_2 rock		123.9	4		123.3	4		108.0	4
Deformation		77.5	18		77.0	18		74.5	18
ClThF bend		66.3	5		66.0	5		57.7	2

[a] Frequencies and calculated intensities are in cm^{-1} and km/mol , calculated using B3LYP/6-311++G(2d,p)/SDD. [b] Observed in argon matrix.

compares the B3LYP calculated and argon matrix observed frequencies for $\text{CH}_2=\text{ThFCl}$, and the agreement is satisfactory. For comparison, we repeated the calculation using the BPW91 pure density functional, and found the same structure with a slightly smaller agostic angle (102.5°) and shorter $\text{C}=\text{Th}$ bond (2.135 \AA), and similar results were found with the PW91 functional.^[15] Analogous behavior has been reported for the $\text{CH}_2=\text{TiHF}$ complex.^[27] It is interesting to note that the hybrid B3LYP functional predicted the D shift (146 cm^{-1}) for the CH_2 wagging mode (observed, 151 cm^{-1}) more closely than either of the two pure density functionals.

The most critical and diagnostic vibrational mode is the C–Th stretching mode, which is also mixed with the CH_2 bending mode, and the calculation's ability to predict this mode is a measure of successful modeling of the electronic structure. The B3LYP calculation for this mostly C–Th stretching mode is 23 cm^{-1} low, 19 cm^{-1} low, and 2 cm^{-1} high for the $\text{CH}_2=\text{ThF}_2$, $\text{CH}_2=\text{ThFCl}$, and $\text{CH}_2=\text{ThCl}_2$ series. The pure density functional BPW91 calculation (Tables S1, S2, and S3, Supporting Information) predicts this mode with about the same accuracy (30 cm^{-1} low, 11 cm^{-1} low, and 5 cm^{-1} high) for these complexes.

We must also point out that the calculations overestimate the intensity of the CH_2 wagging mode relative to the C–Th stretching mode for these methyldene complexes. Part of the problem may be experimental as the wagging mode is broad in the matrix, but nevertheless the integrated intensity of the wagging mode is about half that observed for the C–Th stretching mode in these methyldene complexes.

CHX_3

Thorium and fluoroform gave a strong product absorption at 521.3 cm^{-1} just above the 508 cm^{-1} precursor band, and absorptions at 565.4 and 502.1 cm^{-1} , which are labeled with arrows in Figure 5. These bands increased 10% on $>290 \text{ nm}$ and 20% on $>220 \text{ nm}$ irradiations and shifted slightly with CDF_3 to 520.6 cm^{-1} and to 563.4 and 493.1 cm^{-1} .

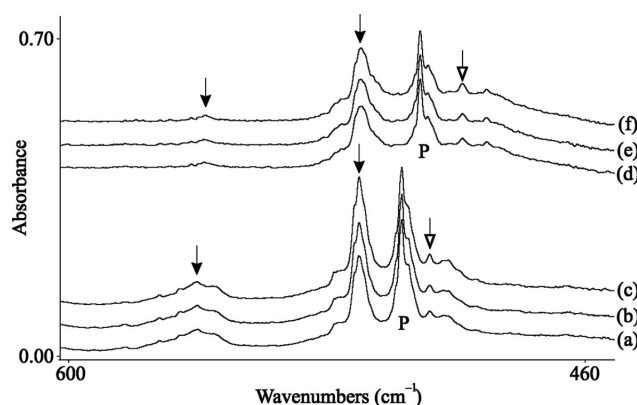
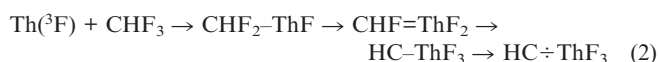


Figure 5. Infrared spectra in the $600\text{--}450 \text{ cm}^{-1}$ region for laser-ablated Th atoms co-deposited with CHF_3 in excess argon at 8 K. (a) Th and 1% CHF_3 in argon co-deposited for 1 h, (b) after $>290 \text{ nm}$ irradiation, (c) after $>220 \text{ nm}$ irradiation, and (d) after annealing to 30 K. (e) Th and 1% CDF_3 in argon co-deposited for 1 h, (f) after $>290 \text{ nm}$ irradiation, (g) after $>220 \text{ nm}$ irradiation, and (h) after annealing to 30 K. P denotes fluoroform precursor absorptions.

Following the example of Group 4 reactions,^[13] the most stable complex with this stoichiometry is triplet $\text{HC}\div\text{ThF}_3$, and the calculated structure is shown in Figure 6. This reaction proceeds through two $\alpha\text{-F}$ transfers after the initial insertion, Equation (2), which is overall 227 kcal/mol exothermic. The $\text{CHF}=\text{ThF}_2$ structural isomer singlet methyldene complex is 46 kcal/mol higher in energy than the final product and an intermediate step in the reaction mechanism. The singlet-state $\text{HC}\text{--}\text{ThF}_3$ product is 30 kcal/mol higher in energy than the global minimum energy triplet, and it may also be an intermediate in the formation of the final triplet state product.



The calculated and observed frequencies are compared in Table 4. The weaker symmetric Th–F stretching frequency predicted at 568.5 cm^{-1} with 2.5 cm^{-1} D shift is in very good agreement with the 565.4 cm^{-1} observed band with 2.1 cm^{-1}

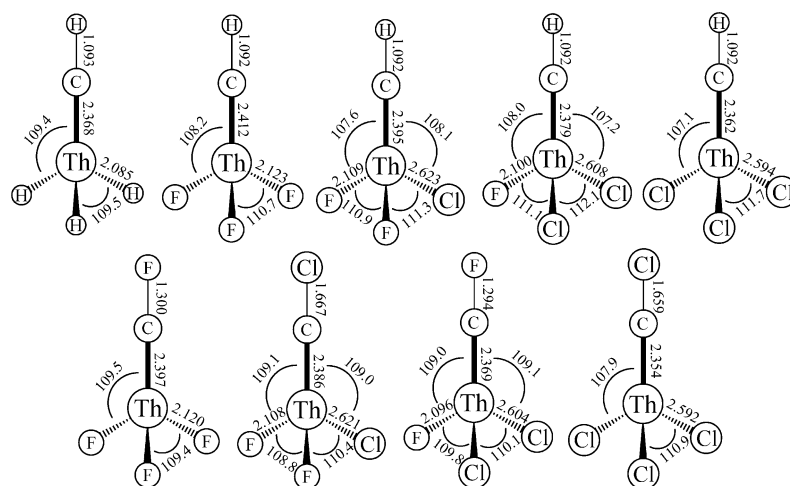


Figure 6. Optimized molecular structures [B3LYP/6-311++G(2d,p)/SDD] for $\text{HC}\div\text{ThX}_3$ and $\text{XC}\div\text{ThX}_3$ complexes ($\text{X} = \text{H}, \text{F}, \text{Cl}$). Bond lengths are in Å and angles are in °.

D shift. The very strong antisymmetric Th–F stretching mode predicted at 526.0 cm^{-1} with 0.3 cm^{-1} D shift is matched by the very strong 521.3 cm^{-1} observed band with 0.7 cm^{-1} D shift. The weaker 502.1 cm^{-1} band with 9.0 cm^{-1} D shift approximates the calculated 508.9 cm^{-1} C–Th stretching mode with 16.6 cm^{-1} D shift: there probably is mixing with the symmetric Th–F stretching mode not accounted for in the calculation. The correlation between three calculated and observed frequencies for $\text{HC}\div\text{ThF}_3$ substantiates this identification and the vibrational assignments.

Table 4. Observed and calculated fundamental frequencies for $\text{HC}\div\text{ThF}_3$ in C_{3v} symmetry in the triplet ground electronic state.^[a]

Approximate	$\text{HC}\div\text{ThF}_3$		$\text{DC}\div\text{ThF}_3$	
Mode	Obsd. ^[b]	Calcd. (Int.)	Obsd. ^[b]	Calcd. (Int.)
C–H stretch, a_1		3108.6 (5)		2288.6 (0)
Th–F stretch, a_1	565.4	568.5 (17)	563.4	566.0 (30)
Th–F stretch, e	521.3	526.0 (419)	520.6	525.7 (404)
C–Th stretch, a_1	502.1	508.9 (180)	493.1	492.3 (160)
H–C–Th bend, e	– ^[c]	425.9 (68)		328.3 (56)
F–Th–F bend, a_1		120.5 (1)		117.4 (4)
F–Th–F bend, e		117.5 (27)		115.4 (27)
C–Th–F bend, e		106.0 (37)		102.0 (17)

[a] Frequencies and intensities are in cm^{-1} and km/mol . Intensities are all calculated values using B3LYP/6-311++G(2d,p)/SDD. [b] Absorptions observed in argon matrix. [c] Absorption falls at the limit of instrumental detection.

Thorium and chloroform produced a new 548.2 cm^{-1} absorption, which doubled on $>290\text{ nm}$ irradiation and increased another 10% on $>220\text{ nm}$ irradiation. This band shifted to 528.0 cm^{-1} with the CDCl_3 reagent and to 529.3 cm^{-1} with the ^{13}C precursor, as shown in Figure 7. Our calculation for $\text{HC}\div\text{ThCl}_3$ predicted one strong absorption, namely the C–Th stretching mode (Table 5), in the observable spectral region at 543.9 cm^{-1} , which is in very good agreement with the new band at 548.2 cm^{-1} . The calculation further predicted a 20.3 cm^{-1} D shift (observed

20.2 cm^{-1}) and an 18.6 cm^{-1} ^{13}C shift (observed 18.9 cm^{-1}). Thorium and bromoform gave a weaker new absorption 1.0 cm^{-1} higher at 549.2 cm^{-1} for the $\text{HC}\div\text{ThBr}_3$ product, and our calculations predict that the C–Th stretching mode should be 2.2 cm^{-1} higher for this complex since the C÷Th bond is stronger (2.352 Å in $\text{HC}\div\text{ThBr}_3$) for the less electronegative halogen substituents. This agreement between calculated and observed isotopic shifts is reassuring to say the least.

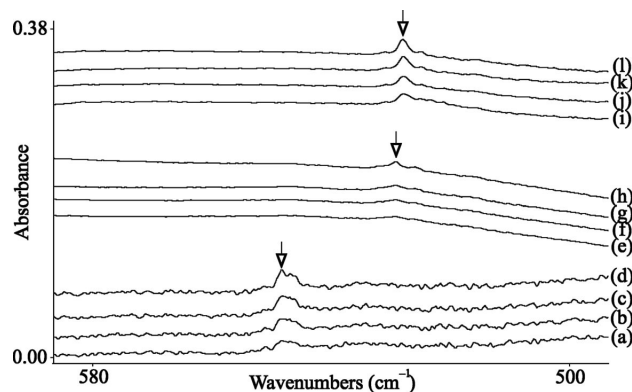


Figure 7. Infrared spectra in the $580\text{--}600\text{ cm}^{-1}$ region for laser-ablated Th atoms co-deposited with CHCl_3 in excess argon at 8 K. (a) Th and 0.5% CHCl_3 co-deposited for 1 h. (b) after $>290\text{ nm}$ irradiation, (c) after $>220\text{ nm}$ irradiation, and (d) after annealing to 30 K. (e) Th and 0.5% $^{13}\text{CHCl}_3$ in argon co-deposited for 1 h, (f) after $>290\text{ nm}$ irradiation, (g) after $>220\text{ nm}$ irradiation, and (h) after annealing to 30 K. (i) Th and 0.5% CDCl_3 in argon co-deposited for 1 h, (j) after $>290\text{ nm}$ irradiation, (k) after $>220\text{ nm}$ irradiation, and (l) after annealing to 30 K.

The mixed haloform refrigerants CHF_2Cl and CHFCl_2 were also investigated to determine the “tuning” effect on the C÷Th bond as the substituent is changed stepwise, and the calculated $\text{HC}\div\text{ThF}_2\text{Cl}$ and $\text{HC}\div\text{ThFCl}_2$ structures are compared in Figure 6 with those for $\text{HC}\div\text{ThF}_3$ and $\text{HC}\div\text{ThCl}_3$. The C÷Th bond length decreases as F is re-

Table 5. Observed and calculated fundamental frequencies for $\text{HC}\div\text{ThCl}_3$ and $\text{HC}\div\text{ThBr}_3$ in C_{3v} symmetry in the triplet ground electronic state.^[a]

Approximate	$\text{HC}\div\text{ThCl}_3$		$\text{H}^{13}\text{C}\div\text{ThCl}_3$		$\text{DC}\div\text{ThCl}_3$		$\text{HC}\div\text{ThBr}_3$	
Mode	Obsd. ^[b]	Calcd. (Int.)	Obsd. ^[b]	Calcd. (Int.)	Obsd. ^[b]	Calcd. (Int.)	Obsd.	Calcd. (Int.)
C–H stretch, a_1		3121 (0)		3111 (1)		2298 (2)		3124 (0)
C–Th stretch, a_1	548.2	543.9 (99)	529.3	525.3 (93)	528.0	523.6 (92)	549.2	546.1 (92)
H–C–Th bend, e	— ^[c]	448 (96)	— ^[c]	445 (96)		348 (138)	— ^[c]	443 (76)
Th–Cl stretch, a_1		324 (28)		324 (28)		324 (27)		223 (112)
Th–Cl stretch, e		321 (206)		321 (106)		318 (138)		205 (10)
Cl–Th–Cl bend, a_1		97 (2)		95 (2)		91 (1)		90 (0)
Cl–Th–Cl bend, e		66 (6)		66 (6)		66 (6)		45 (4)
C–Th–Cl bend, e		62 (9)		62 (9)		62 (9)		43 (2)

[a] Frequencies and intensities are in cm^{-1} and km/mol . Intensities are all calculated values using B3LYP/6-311++G(2d,p)/SDD. [b] Absorptions observed in argon matrix. [c] Absorption falls at the limit of instrumental detection.

Table 6. Observed and calculated fundamental frequencies for $\text{HC}\div\text{ThF}_2\text{Cl}$ and $\text{HC}\div\text{ThFCl}_2$ in C_s symmetry in the triplet ground electronic state.^[a]

$\text{HC}\div\text{ThF}_2\text{Cl}$			$\text{HC}\div\text{ThFCl}_2$		
Mode	Obsd. ^[b]	Calcd. (Int.)	Mode	Obsd. ^[b]	Calcd. (Int.)
C–H stretch, a'		3113.5 (3)	C–H stretch, a'		3117.1 (1)
Th–F stretch, a'	563.4 ^[c]	563.6 (82)	Th–F stretch, a'	557.7 ^[e]	560.6 (126)
Th–F stretch, a''	531.1 ^[c]	535.8 (196)	C–Th stretch, a'	531.1 ^[e]	531.3 (138)
C–Th stretch, a'	521.6 ^[c]	518.7 (160)	Th–C–H bend, a''	— ^[d]	439.7 (50)
Th–C–H bend, a'	— ^[d]	433.5 (46)	Th–C–H bend, a'	— ^[d]	439.3 (39)
Th–C–H bend, a''		431.6 (34)	Th–Cl stretch, a'		318.6 (50)
Th–Cl stretch, a'		312.5 (83)	Th–Cl stretch, a''		315.9 (111)
C–Th–F bend, a''		123.8 (10)	C–Th–F, bend, a'		115.3 (6)

[a] Frequencies and intensities are in cm^{-1} and km/mol . Intensities are all calculated values using B3LYP/6-311++G(2d,p)/SDD. [b] Absorptions observed in argon matrix. [c] The ^{13}C counterparts were observed at 561.5, 531.0, and 506.9 cm^{-1} , and the calculated values are 561.3, 535.7, and 503.1 cm^{-1} . [d] Absorption falls below the limit of instrumental detection. [e] The D counterparts were observed at 552.5 and 517.7 cm^{-1} , and the calculated values are 558.6 and 513.3 cm^{-1} .

placed by Cl on the thorium center. The reaction of Th and CHF_2Cl gave new absorptions at 563.4, 531.1, and 521.6 cm^{-1} , and the analogous reaction with CHFCl_2 produced a strong band at 557.7 cm^{-1} and a weaker band at 531.1 cm^{-1} . Calculated frequencies are compared in Table 6, and the agreement is within a few wavenumbers. Notice that the calculated frequencies correlate and that the observed bands are all in the same region. The new product peaks are labeled with solid arrows (for Th–F stretching modes following the fluoroform product) and open arrows (for C–Th stretching modes following the chloroform product) in Figure 8. The two Th–F stretching modes for $\text{HC}\div\text{ThF}_2\text{Cl}$ at 563.4 and 531.1 cm^{-1} are very near these two modes for $\text{HC}\div\text{ThF}_3$ at 565.4 and 521.3 cm^{-1} , as can reasonably be expected. Likewise the single Th–F stretching mode for $\text{HC}\div\text{ThFCl}_2$ at 557.7 cm^{-1} is intermediate between the pairs of symmetric and antisymmetric Th–F stretching modes. Isotopic samples were available for $^{13}\text{CHF}_2\text{Cl}$ and CDFCl_2 , the shifts are compared in Table 6 as footnotes: the calculated and observed shifts agree well enough to substantiate our vibrational assignments.

It is perhaps of more interest to follow the C–Th stretching mode in $\text{HC}\div\text{ThF}_3$ as F is replaced stepwise with Cl and the C–Th bond length decreases (Figure 6). The observed bands labeled with open arrows increase from 502.1 to 521.6 to 531.1 to 548.2 cm^{-1} in Figure 8 from bottom to top. The observed trend is in agreement with our calcula-

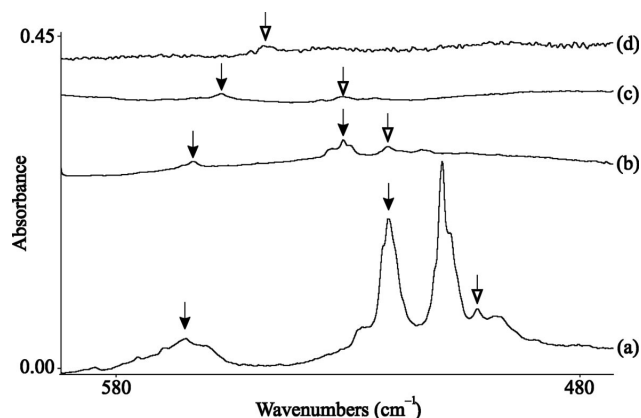


Figure 8. Infrared spectra in the 580–490 cm^{-1} region for laser-ablated Th atoms co-deposited and reacted with haloform precursors in excess argon at 8 K for 1 h. (a) Th and CHF_3 , (b) Th and CHF_2Cl , (c) Th and CHFCl_2 , and (d) Th and CHCl_3 .

tions as this bond is calculated to be slightly shorter in the chlorine species and the frequency higher (Tables 4 and 5). Furthermore, the calculation predicts the mode for the chlorine species more accurately in position and isotopic shifts than for the fluorine species. This again underscores the difficulty in accurately calculating molecules containing fluorine particularly where the mixing of nearby vibrational modes is concerned.

CX₄

The CF₄ reagent and Th produced a strong 521.7 cm⁻¹ band and a weaker 563.4 cm⁻¹ absorption. These bands increased slightly with >290 nm irradiation and 30–60% with >220 nm irradiation as shown in Figure 9. The CF₂Cl₂ precursor gave strong bands at 556.1 and 534.8 cm⁻¹ and weaker bands at 1328.6 and 553.6 cm⁻¹ labeled B and A, respectively, according to the notation for the Group 4 reaction products. These bands were not affected by >290 nm irradiation, but they increased 25% with >220 nm irradiation. The higher band shifted with ¹³CF₂Cl₂ probably falling under a common band at 1294 cm⁻¹, but the lower bands were unchanged. Thorium and CF₃Cl gave three new site-split doublets at 557.5, 554.0 cm⁻¹, at 534.1, 531.2 cm⁻¹, and at 524.5, 521.6 cm⁻¹, and the ¹³CF₃Cl reagent produced no shifts. Finally, the reaction with CCl₄ produced no observable absorptions above 440 cm⁻¹.

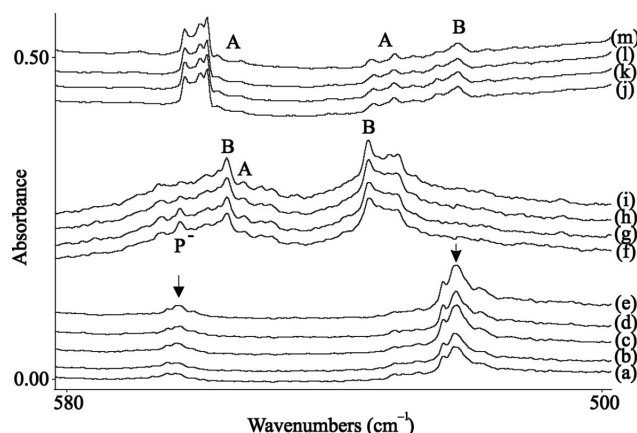


Figure 9. Infrared spectra in the 580–500 cm⁻¹ region for laser-ablated Th atoms co-deposited with CX₄ precursors in excess argon at 8 K. (a) Th and 0.2% CF₄ in argon co-deposited for 1 h, (b) after >290 nm irradiation, (c) after >220 nm irradiation, (d) after annealing to 30 K, and (e) after a second >220 nm irradiation. (f) Th and 0.2% CF₂Cl₂ in argon co-deposited for 1 h, (g) after >290 nm irradiation, (h) after >220 nm irradiation, and (i) after annealing to 30 K. (j) Th and 0.2% CF₃Cl in argon co-deposited for 1 h, (k) after >290 nm irradiation, (l) after >220 nm irradiation, and (m) after annealing to 30 K. P denotes precursor and P⁻ precursor anion absorptions.

The two bands observed with CF₄ at 563.4 and 521.7 cm⁻¹ are almost the same as the above HC÷ThF₃ product absorptions at 565.4 and 521.3 cm⁻¹, and a similar FC÷ThF₃ structure is suggested. The frequencies calculated for the analogous HC÷ThF₃ product compared in Table 4 are only a few cm⁻¹ different. Unfortunately, the diagnostic high-frequency C–F stretching mode predicted at 1330.5 cm⁻¹ is masked by the totally absorbing precursor absorption at 1330–1240 cm⁻¹. The calculated structures of triplet HC÷ThF₃ and FC÷ThF₃ are compared in Figure 6. Note the common structural features. The singlet-state analogs in each case have slightly different structures. The singlet HC–ThF₃ is 30 kcal/mol higher in energy, has the same (2.412 Å) C–Th bond length, and a 178.6° bond angle. The singlet FC–ThF₃ is 25 kcal/mol higher in energy, but has a slightly longer (2.401 Å) C–Th bond, almost the same Th–F bond length, but different F–Th–F angles (98.6, 113.4, and 115.2°).

The FC÷ThF₃ complex is formed by the straightforward reaction (3), where the triplet CF₂–ThF₂ methyldene complex is 179 kcal/mol lower in energy than the Th + CF₄ reagents, and the final triplet FC÷ThF₃ complex is 230 kcal/mol more stable than the reagents. The analogous singlet-state FC–ThF₃ complex has a similar computed spectrum but is 25 kcal/mol higher in energy and has a slightly longer (2.401 Å) C–Th bond. Even though the triplet CF₂–ThF₂ complex is isoergic with the singlet CF₂=ThF₂ complex, the former has a much longer (2.471 Å) C–Th bond. Therefore, reaction (3) probably proceeds on the triplet potential energy surface. The analogous reaction with CCl₄ is presumed to go likewise, but no product absorptions were observed: the Th–Cl stretching frequencies are lower than our cutoff (Table 7), and the C–Cl stretch is weak and probably covered by one of the transient species absorptions near 1000 cm⁻¹.



The two different α -halogen transfer products are observed with CF₂Cl₂ just as found with the Group 4 metals.^[14] First notice the two strongest bands at 556.1 and 534.8 cm⁻¹, which fall between the two absorptions for the FC÷ThF₃ complex and are appropriate for two Th–F stretching modes for the ClC÷ThF₂Cl complex labeled B.

Table 7. Observed and calculated fundamental frequencies for FC÷ThF₃ and ClC÷ThCl₃ in C_{3v} symmetry in the triplet ground electronic state.^[a]

Approximate Mode	FC÷ThF ₃ Obsd. ^[b]	Calcd. (Int.)	F ¹³ C÷ThF ₃ Calcd. (Int.)	ClC÷ThCl ₃ Calcd. (Int.)
C–X stretch, a ₁	— ^[c]	1330.5 (174)	1294.3 (172)	1026 (12)
Th–X stretch, a ₁	563.4	563.4 (85)	563.3 (86)	325 (39)
Th–X stretch, e	521.7	527.8 (393)	527.8 (393)	322 (225)
XC–Th stretch, a ₁		330.4 (91)	327.0 (89)	265 (67)
X–C–Th bend, e		195.7 (26)	189.3 (25)	175 (14)
X–Th–X bend, a ₁		120.0 (1)	120.0 (22)	66 (4)
X–Th–X bend, e		116.4 (23)	116.4 (23)	61 (8)
C–Th–X bend, e		77.9 (11)	77.9 (11)	40 (2)

[a] Frequencies and intensities are in cm⁻¹ and km/mol. Intensities are all calculated values using B3LYP/6-311+G(2d)/SDD. [b] Absorptions observed in argon matrix. [c] Absorption masked by intense precursor band.

These bands showed no ^{13}C shift. We also observe a 1328.6 cm^{-1} band for species A, which probably shifts 34 cm^{-1} with ^{13}C as is expected for a C–F stretching mode, but a common precursor band prevents this observation, and the associated 553.6 cm^{-1} band for a Th–F stretching mode. This C–F stretching absorption is lower than the analogous 1428.4 cm^{-1} band for the $\text{FC}\div\text{ZrFCl}_2$ complex, which exhibits a 2.74% ^{13}C shift. Interestingly the C–F bond (1.278 \AA) is shorter in the $\text{FC}\div\text{ZrFCl}_2$ complex than in the present $\text{FC}\div\text{ThFCl}_2$ complex (1.294 \AA), and the lower C–F stretching frequency for the latter is appropriate. Apparently, the longer (2.368 \AA) and weaker C–Th bond does not support as much conjugation with the adjacent C–F bond as does the shorter (2.122 \AA) and stronger C–Zr bond.

The bond stretching frequencies calculated for the $\text{FC}\div\text{ThFCl}_2$ and $\text{ClC}\div\text{ThF}_2\text{Cl}$ complexes are listed in Table S4 (Supporting Information). The only frequency that shows a significant ^{13}C shift is the C–F stretching mode (37.0 cm^{-1}) and the C–Cl stretching mode (33.5 cm^{-1}), which is not observed for the latter due to masking by a precursor fragment absorption in this region. The two modes measured for the former complex A are C–F and Th–F stretching, and the two observed for the latter complex B are both Th–F stretching modes. The latter complex is 11 kcal/mol more stable than the former complex,

and the yield of the lower energy complex with more α -F transfer dominates the product spectrum analogous to results found for Zr and Hf.^[14]

The strongest band at 521.6 cm^{-1} labeled B in Figure 9 from the reaction with CF_3Cl is assigned to essentially the antisymmetric Th–F stretching mode of the $\text{ClC}\div\text{ThF}_3$ complex, and the weaker symmetric counterpart predicted about 34 cm^{-1} higher is masked by the precursor absorption. The weaker matched pairs at 557.5 , 554.0 cm^{-1} and at 534.1 , 531.2 cm^{-1} labeled A are assigned to the $\text{FC}\div\text{ThF}_2\text{Cl}$ isomer based on agreement with our calculations (Table S5, Supporting Information): the observed absorptions did not shift with the $^{13}\text{CF}_3\text{Cl}$ precursors, which is appropriate for Th–F stretching modes. Unfortunately, the C–F stretching mode is masked by another precursor absorption. The two Th–F stretching modes for the latter complex are almost the same as these modes for the $\text{ClC}\div\text{ThF}_2\text{Cl}$ complex with common ThF_2Cl subgroups. Note how closely the frequencies agree for these related complexes in Tables 7 and S4 (Supporting Information). Again, the more stable $\text{ClC}\div\text{ThF}_3$ complex (by 10 kcal/mol) with more α -F transfer is stronger in the spectrum than the isomer $\text{FC}\div\text{ThF}_2\text{Cl}$. The structural parameters for these complexes are given in Table 8, and the same halogen substituent effect on the $\text{ClC}\div\text{ThF}_2\text{Cl}$ bond found with CF_2Cl_2 is again noted with the CF_3Cl precursor.

Table 8. Structural parameters and physical constants of ground-state $\text{X}^1\text{C}\div\text{ThX}_2$ ($\text{X} = \text{H, F, Cl}$).^[a]

Parameter	$\text{HC}\div\text{ThF}_3$	$\text{HC}\div\text{ThCl}_3$	$\text{FC}\div\text{ThF}_3$	$\text{ClC}\div\text{ThCl}_3$	$\text{FC}\div\text{ThFCl}_2$	$\text{ClC}\div\text{ThF}_2\text{Cl}$	$\text{FC}\div\text{ThF}_2\text{Cl}$	$\text{ClC}\div\text{ThF}_3$
$r(\text{C}-\text{X}^1)$	1.092	1.092	1.300	1.659	1.294	1.667	1.297	1.670
$r(\text{C}\div\text{M})$	2.412	2.362	2.397	2.354	2.369	2.386	2.383	2.402
$r(\text{M}-\text{X}^2)$	2.123	2.594	2.120	2.592	2.096/2.604	2.108/2.621	2.106/2.622	2.120
$\angle(\text{CMX}^2)$	108.2	107.1	109.5	107.9	109.0/109.1	109.1/109.0	109.2/110.4	109.0
$\angle(\text{X}^2\text{MX}^2)$	110.7	111.7	109.4	110.9	109.8/110.1	108.8/110.4	107.6/110.3	109.9
$q(\text{X}^1)^{[\text{b}]}$	0.147/0.105	0.136/0.116	−0.223/−0.343	0.149/0.119	−0.210/	0.139/	−0.216/	0.126/
$q(\text{C})^{[\text{b}]}$	−0.870/−0.844	−0.899/−0.804	−0.481/−0.358	−0.750/−0.847	−0.523/	−0.826/	−0.511/	−0.857/
$q(\text{M})^{[\text{b}]}$	2.193/3.114	2.479/2.696	2.158/3.069	2.747/2.729	2.387/	2.309/	2.286/	2.179/
$q(\text{X}^2)^{[\text{b}]}$	−0.490/−0.792	−0.572/−0.669	−0.485/−0.790	−0.715/−0.667	−0.452/	−0.468/	−0.466/	−0.483/
$q(\text{X}^2)^{[\text{b}]}$	—	—	—	—	−0.602/	−0.686/	−0.626/	—
$\text{X}^1(\text{s})^{[\text{c}]}$	0.89	0.88	1.84	1.82				
$\text{X}^1(\text{p})^{[\text{c}]}$	—	—	5.47	5.01				
$\text{C}(\text{s})^{[\text{c}]}$	1.66	1.64	1.62	1.64				
$\text{C}(\text{p})^{[\text{c}]}$	3.18	3.15	2.69	3.17				
$\text{Th}(\text{s})^{[\text{c}]}$	0.09	0.21	0.08	0.20				
$\text{Th}(\text{d})^{[\text{c}]}$	0.38	0.58	0.39	0.56				
$\text{Th}(\text{f})^{[\text{c}]}$	0.40	0.49	0.44	0.48				
$\text{X}^2(\text{s})^{[\text{c}]}$	1.97	1.96	1.97	1.96				
$\text{X}^2(\text{p})^{[\text{c}]}$	5.81	5.69	5.81	5.69				
$s(\text{X}^1)^{[\text{d}]}$	−0.074	−0.070	0.107	0.227	0.112	0.217	0.110	0.211
$s(\text{C})^{[\text{d}]}$	1.874	1.826	1.577	1.492	1.537	1.537	1.557	1.561
$s(\text{M})^{[\text{d}]}$	0.171	0.193	0.286	0.248	0.311	0.217	0.298	0.200
$s(\text{X}^2)^{[\text{d}]}$	0.009	0.017	0.010	0.011	0.010	0.009	0.010	0.009
$s(\text{X}^2)^{[\text{d}]}$	—	—	—	—	0.015	0.010	0.015	—
$\mu^{[\text{e}]}$	1.050	1.940	0.493	2.015	1.508	1.621	1.283	0.748
$\Delta E^{[\text{f}]}$	227	227	230	246	238	249	235	245

[a] Bond lengths and angles are in \AA and $^\circ$. All calculations performed at the B3LYP//6-311++G(2d,p)/SDD level. Halogens denoted by X are given superscripts depicting their position (see Table title). If two different halogen atoms are in the X^2 position (in Freon-12 and -13 experiments), parameters involving more fluorine atoms are given before chlorine. [b] Mulliken atomic/Natural charges. [c] Natural electron configuration for valence orbitals. [d] Mulliken atomic spin densities. [e] Molecular dipole moment in D . [f] Binding energy in kcal/mol relative to $\text{M} + \text{CHX}_3$ or CX_4 .

Bonding and Family Trends

Thorium forms methyldiene complexes in reactions with methane and methyl halides, and the agostic structures of $\text{CH}_2=\text{ThH}_2$ and $\text{CH}_2=\text{ThHF}$ are comparable to those of the related methyldiene Group 4 complexes.^[8–10] The $\text{CH}_2=\text{Th}$ subunit is almost coplanar, but the H and F atoms on the Th atom are out of this plane. The agostic distortion of the CH_2 group to place one H atom much closer to the Th atom than the other one results in an agostic H–C–Th angle near 95° and helps to stabilize the C=Th double bond (2.116 Å and 2.129 Å) in these first investigated (methyldiene)actinide complexes. The $\text{CH}_2=\text{ThF}_2$ complex is computed to be approximately symmetrical at the B3LYP level but CH_2 -distorted using pure density functionals with the ThX_2 group out of the $\text{CH}_2=\text{Th}$ plane in all calculations performed. It was suggested for the Group 4 analogs that this lack of agostic distortion may be due to balanced lone-pair repulsions on the two symmetrical halogen substituents.^[13] Note in Figure 2 that the C=Th bond length increases with the number of fluorine substituents as the π -bonding interaction decreases presumably due to the inductive effect of the fluorine atoms contracting the Th 6d orbitals to make them less effective in π -bonding with the carbon atom. This C=Th bond length increase is substantial for $\text{CF}_2=\text{ThF}_2$, and the complex is less distorted. Note, however, that the $\text{CHF}=\text{ThF}_2$ complex is distorted in the converged minimum-energy structure. This highlights the delicate balance between non-bonded interactions and substituent effects on the orbital overlap that can contribute to the molecular structure. The mixed complex $\text{CH}_2=\text{ThFCl}$ is distorted and the C–Th bond length is also intermediate between the difluoro and dichloro complex values. The final complex illustrated, $\text{CH}_2=\text{ThCl}_2$, is more distorted in the converged minimum, whereas the Group 4 analogs were found to be symmetrical.^[12] Here, the C–Th bond is shorter than for the fluorine analog because the inductive effect of chlorine atoms is less, such that the Th 6d orbital overlap with the C 2p orbital is better and the agostic interaction comes into play. Note that the C–Th stretching frequencies increase steadily in this series as the bond length decreases.

Thorium forms very stable triplet-state electron-deficient $\text{HC}\div\text{ThF}_3$ and $\text{FC}\div\text{ThF}_3$ methyldiene complexes analogous to the Group 4 metals.^[11–14] The spin densities on Th are comparable to those for Zr, which indicates similar small electron transfer from the carbon atom to the metal center in the degenerate pair of singly occupied molecular orbitals (SOMO) with the resulting weak π -bonding interaction. Apparently, the relativistic contraction^[29] for Th 6d orbitals improves their overlap with C 2p orbital over that for the Hf 5d orbital to be nearly the same as the Zr 4d orbitals. However, the C \div Th bond is considerably longer than the Group 4 C \div M bonds, and the common C–H and C–X bonds are also longer in the thorium complexes. This means that the C–F conjugation with the C \div Ti bond proposed to explain the very high C–F stretching frequency^[11] is diminished in the Th complexes, and as a consequence, the C–F stretching frequency moves down about 140 cm^{-1}

(calculated) where it is now covered by the massive CF_4 absorption. However, the C–F stretching mode in the $\text{FC}\div\text{ThFCl}_2$ complex is observed here at 1328.6 cm^{-1} compared to $\text{FC}\div\text{ZrFCl}_2$ at 1428.4 cm^{-1} , and the calculated difference is 111 cm^{-1} . As found for Group 4 metals,^[14] we again observe that chlorine substitution for fluorine at both carbon and metal positions (Figure 6) fosters electron transfer from the carbon atom to the metal center in the doubly degenerate SOMO pair and enhances the π -bonding interaction in these electron-deficient methyldiene complexes. Likewise, the C–Cl conjugation with the carbon–thorium bond is diminished relative to the carbon–titanium case.^[11]

Notice that the C \div Th bond is shorter in $\text{HC}\div\text{ThH}_3$ and $\text{HC}\div\text{ThCl}_3$ than in $\text{HC}\div\text{ThF}_3$, which is due at least in part to the more electronegative fluorine substituent increasing the positive charge at the metal center and concentrating the Th 6d and 5f orbitals making them slightly less effective in overlapping with C 2p orbitals. The spin densities (Table 8) show that more electron density is transferred from C to Th in the chlorine compound. This happens stepwise in the $\text{HC}\div\text{ThF}_3$ to $\text{HC}\div\text{ThF}_2\text{Cl}$ to $\text{HC}\div\text{ThFCl}_2$ to $\text{HC}\div\text{ThCl}_3$ series (Figure 6). In addition notice the substantially increased Th 6d and 5f contributions to the natural electron configurations from Natural Bond Order analysis^[30] in the chlorine species. There is a significant Th 5f orbital participation in the doubly degenerate SOMOs responsible for the weak π -bonding. A similar substantial participation of Th 5f orbitals in π -bonding to a first-row element has been reported recently for $\text{HN}=\text{ThH}_2$.^[31] In addition, the mixing of Th 5f orbitals into the valence shell has been suggested to enhance the ability of Th to activate methane.^[32]

An interesting comparison is in the Th + CF_4 family of products, singlet $\text{CF}_2=\text{ThF}_2$, triplet $\text{FC}\div\text{ThF}_3$, singlet $\text{FC}-\text{ThF}_3$, and triplet CF_2-ThF_2 , which suffer from the same inductive effect of four fluorine substituents and have C–Th bond lengths of 2.262 Å, 2.397 Å, 2.401 Å, and 2.471 Å, respectively, computed at the B3LYP level of theory. The effect of the two SOMOs in triplet $\text{FC}\div\text{ThF}_3$ then is found to be less than that of a shared π -bond but reduces the C–Th bond length slightly from singlet $\text{FC}-\text{ThF}_3$ and substantially from triplet CF_2-ThF_2 .

It is clear that these methyldiene structures are thermodynamically favored with at least three halogen atoms in the methane precursor owing to the great stability of the metal–halide bond. For example, $\text{FC}\div\text{ThF}_3$ is 51 kcal/mol lower in energy than $\text{CF}_2=\text{ThF}_2$, but $\text{HC}\div\text{ThH}_3$ is 41 kcal/mol higher in energy than $\text{CH}_2=\text{ThH}_2$, even though the C \div Th bond is slightly shorter in the hydride complex (Figure 6).

Another interesting comparison is between the $\text{FC}\div\text{ThF}_3$ and $\text{HC}\div\text{ThF}_3$ molecules. It is clear that the delocalized π -bonding in $\text{FC}\div\text{ThF}_3$ is greater than in $\text{HC}\div\text{ThF}_3$ based on computed bond lengths (2.397 Å, 2.412 Å) and spin densities on C and Th (1.577, 0.286; 1.874, 0.171), respectively, and that the latter is more ionic (natural charges for Th, C are 3.11, –0.84) than the former

(3.07, -0.36) (see Table 8). The same relationship was found for $\text{ClC}\div\text{ThCl}_3$ and $\text{HC}\div\text{ThCl}_3$ and the analogous Group 4 molecules. Apparently, the halogen substituent on the carbon atom withdraws sufficient electron density to contract the C 2p orbitals and to make for more favorable overlap with the metal valence d orbitals and accordingly to increase the X–C π -bonding in these systems. The natural electron configurations (Table 8) show substantially less carbon 2p character for the FC than for the HC and ClC derivatives. Although the singlet analogs $\text{FC}\div\text{ThF}_3$ and $\text{HC}\div\text{ThF}_3$ are 25 and 30 kcal/mol higher in energy, the C–Th bond is only slightly longer, 2.401 Å in the first case, and the same, 2.412 Å in the second case, relative to the triplet states, so the degenerate SOMOs contribute a small amount of delocalized π -bonding to the final triplet-state products. One of the SOMOs is illustrated in Figure 10: notice that the SOMO has slight contact with Th and extends past C and even H. However, when two more electrons are added to the system, as in the $\text{FC}\equiv\text{UF}_3$ and $\text{HC}\equiv\text{UF}_3$ (methylidyne)uranium molecules, the six-electron $\text{C}\equiv\text{U}$ triple bonds are computed to be substantially shorter, 2.007 Å and 1.941 Å, respectively.^[33] In this (methylidyne)-uranium system, there is more HOMO contact with U and only slight extension past C.

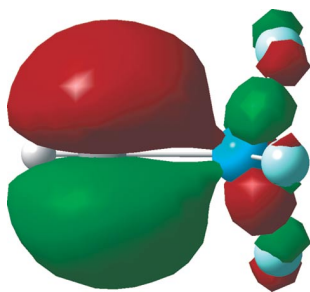


Figure 10. One of the degenerate SOMOs in $\text{HC}\div\text{ThF}_3$ plotted with an iso-electron density of 0.02.

Conclusions

Laser-ablated Th atoms react with methylene halides to form the (methylidene)actinide complexes $\text{CH}_2=\text{ThX}_2$ ($\text{X}_2=\text{F}_2$, FCl, Cl_2) as major products trapped in solid argon. These molecules are identified through the effect of isotopic (^{13}C , D) substitution on the infrared spectra and comparison to frequencies and isotopic shifts calculated by density functional theory. The B3LYP-computed structure for the $\text{CH}_2=\text{ThF}_2$ complex shows no evidence of agostic distortion, which is the same found for the analogous Group 4 complexes, but calculations suggest that the $\text{CH}_2=\text{ThFCl}$ complex is distorted and the $\text{CH}_2=\text{ThCl}_2$ complex is more distorted. However, two pure density functionals find distortion for $\text{CH}_2=\text{ThF}_2$ and the same structural trend.

Thorium forms electron-deficient methylidyne $\text{HC}\div\text{ThF}_3$ and $\text{FC}\div\text{ThF}_3$ complexes that are analogous to those of Group 4 with Zr providing the closest approximation to Th.^[12–14] However, the C–M, C–H, and C–F

bonds are longer in the thorium complexes, which suggests that the C–F conjugation with the $\text{C}\div\text{Th}$ bond offered to justify the very high C–F stretching frequency^[11] is decreased in the (methylidyne)thorium complexes. Indeed, the observed spectrum for the $\text{FC}\div\text{ThFCl}_2$ complex shows that this is the case. Like that found for Group 4, chlorine substitution at both carbon and metal positions supports stronger carbon–metal bonding. There is a substantial contribution from Th 5f orbitals in addition to 6d orbitals in the doubly degenerate SOMOs forming the weak singly occupied π -bonds in these electron-deficient methylidyne complexes. Finally, the delocalized π -bonding in $\text{FC}\div\text{ThF}_3$ is greater than in $\text{HC}\div\text{ThF}_3$, which probably arises from contraction of the C 2p orbitals by the fluorine substituent and better overlap with the Th 6d orbitals.

Supporting Information (see footnote on the first page of this article): Tables S1, S2 and S3 containing BPW91 frequency calculations and Tables S4 and S5 containing B3LYP frequency calculations.

Acknowledgments

We gratefully acknowledge financial support for this research from the National Science Foundation.

- [1] R. R. Schrock, *Chem. Rev.* **2002**, 102, 145.
- [2] J. W. Herndon, *Coord. Chem. Rev.* **2004**, 248, 3.
- [3] J. W. Herndon, *Coord. Chem. Rev.* **2005**, 249, 999.
- [4] J. W. Herndon, *Coord. Chem. Rev.* **2006**, 250, 1889.
- [5] J. A. Pool, B. L. Scott, J. L. Kiplinger, *J. Am. Chem. Soc.* **2005**, 127, 1338.
- [6] See for example: R. E. Cramer, R. B. Maynard, J. C. Paw, J. W. Gilje, *J. Am. Chem. Soc.* **1981**, 103, 3589.
- [7] M.-Y. He, G. Xiong, P. J. Toscano Jr, R. L. Burwell, T. J. Marks, *J. Am. Chem. Soc.* **1985**, 107, 641.
- [8] L. Andrews, H.-G. Cho, *J. Phys. Chem. A* **2005**, 109, 6796 (Th + CH_4).
- [9] J. T. Lyon, L. Andrews, *Inorg. Chem.* **2005**, 44, 8610 (Th + CH_3X).
- [10] L. Andrews, H.-G. Cho, *Organometallics* **2006**, 25, 4040 (review article).
- [11] J. T. Lyon, L. Andrews, *Inorg. Chem.* **2006**, 45, 9858 (Ti + CF_4).
- [12] J. T. Lyon, L. Andrews, *Organometallics* **2007**, 26, 332 (Gr 4 + CH_2Cl_2).
- [13] a) J. T. Lyon, L. Andrews, *Organometallics* **2006**, 25, 1341; b) J. T. Lyon, L. Andrews, *Inorg. Chem.* **2007**, 46, 4799 (Gr 4 + CH_2F_2).
- [14] J. T. Lyon, L. Andrews, *Organometallics* **2007**, 26, 2519 (Gr 4 + CF_2Cl_2).
- [15] H.-S. Hu, J. Li, J. T. Lyon, L. Andrews, *Angew. Chem. Int. Ed.* **2007**, 47, 9045.
- [16] P. F. Souter, G. P. Kushto, L. Andrews, M. Neurock, *J. Phys. Chem. A* **1997**, 101, 1287 (Th + H_2).
- [17] L. Andrews, A. Citra, *Chem. Rev.* **2002**, 102, 885, and references therein.
- [18] M. J. Frisch, G. W. Trucks, H. B. Schlegel, G. E. Scuseria, M. A. Robb, J. R. Cheeseman, V. G. Zakrzewski, J. A. Montgomery Jr, R. E. Stratmann, J. C. Burant, S. Dapprich, J. M. Millam, A. D. Daniels, K. N. Kudin, M. C. Strain, O. Farkas, J. Tomasi, V. Barone, M. Cossi, R. Cammi, B. Mennucci, C. Pomelli, C. Adamo, S. Clifford, J. Ochterski, G. A. Petersson, P. Y. Ayala, Q. Cui, K. Morokuma, N. Rega, P. Salvador, J. J. Dannenberg, D. K. Malick, A. D. Rabuck, K. Raghavachari, J. B. Foresman, J. Cioslowski, J. V. Ortiz, A. G. Baboul, B. B. Stefanov, G. Liu, A. Liashenko, P. Piskorz, I. Komaromi, R.

- Gomperts, R. L. Martin, D. J. Fox, T. Keith, M. A. Al-Laham, C. Y. Peng, A. Nanayakkara, M. Challacombe, P. M. W. Gill, B. Johnson, W. Chen, M. W. Wong, J. L. Andres, C. Gonzalez, M. Head-Gordon, E. S. Replogle, J. A. Pople, *Gaussian 98*, revision A.11.4, Gaussian, Inc., Pittsburgh, PA, **2002**.
- [19] a) M. J. Frisch, J. A. Pople, J. S. Binkley, *J. Chem. Phys.* **1984**, *80*, 3265.
- [20] W. Küchle, M. Dolg, H. Stoll, H. Preuss, *J. Chem. Phys.* **1994**, *100*, 7535.
- [21] T. G. Carver, L. Andrews, *J. Chem. Phys.* **1969**, *50*, 5100.
- [22] L. Andrews, F. T. Prochaska, *J. Chem. Phys.* **1979**, *70*, 4714 and references cited therein.
- [23] M. E. Jacox, D. E. Milligan, *J. Chem. Phys.* **1969**, *50*, 3252.
- [24] R. J. M. Konings, *J. Chem. Phys.* **1996**, *105*, 9379.
- [25] A. P. Scott, L. Radom, *J. Phys. Chem.* **1996**, *100*, 16502.
- [26] I. Bytheway, M. W. Wong, *Chem. Phys. Lett.* **1998**, *282*, 219.
- [27] G. von Frantzius, R. Streubel, K. Brandhorst, J. Grunenberg, *Organometallics* **2006**, *25*, 118.
- [28] B. O. Roos, R. H. Lindh, H.-G. Cho, L. Andrews, *J. Phys. Chem. A* **2007**, *111*, 6420 (theoretical study of CH₂=MH₂ complexes).
- [29] P. Pyykko, *Chem. Rev.* **1988**, *88*, 563.
- [30] A. E. Reed, L. A. Curtiss, F. Weinhold, *Chem. Rev.* **1988**, *88*, 899.
- [31] X. Wang, L. Andrews, C. Marsden, *Chem. Eur. J.* **2007**, *13*, 5601 (Th + NH₃).
- [32] K. J. De Almeida, A. Cesar, *Organometallics* **2006**, *25*, 3407.
- [33] J. T. Lyon, H.-S. Hu, L. Andrews, J. Li, *Proc. Natl. Acad. Sci.* **2007**, *104*, 18919.

Received: September 26, 2007

Published Online: December 6, 2007